

## Growth and Optical, Thermal and Electrical Characterization of LHC-LHB Mixed Crystals

J. Suja Rani<sup>\*</sup>, K. Jaya kumari<sup>\*\*</sup>, and C. K. Mahadevan<sup>\*\*\*</sup>

<sup>\*</sup>Department of Physics, Lekshmiapuram college of Arts and Science, Neyyor – 629 802, India

<sup>\*\*</sup>Department of Physics, Sree Ayappa College for Women, Chunkankadai – 629 801, India

<sup>\*\*\*</sup>Department of Physics, S.T. Hindu college, Nagercoil – 629 002, India

### ABSTRACT

Mixed crystals of L-Histidine Hydrochloride-bromide (abbreviated as LHC-LHB), semi organic nonlinear optical (NLO) materials, have been successfully grown by the slow solvent evaporation technique at room temperature. Transparent crystals were obtained over a period of 25 days. The ten grown crystals were characterized structurally, optically, thermally, mechanically and electrically. Lattice parameters of the grown crystals were determined by single crystal X-ray diffraction analysis. UV-Vis-NIR spectra were recorded to estimate the UV cut-off wavelength and transmission range. Second harmonic generation study confirms the NLO property. Thermal stability and decomposition of the crystals have been studied by TG/DTA analysis. Micro hardness measurement indicates that all the crystals grown exhibit normal indentation size effect. The frequency and temperature dependence of dielectric constant ( $\epsilon_r$ ), dielectric loss ( $\tan \delta$ ) and AC conductivity ( $\sigma_{ac}$ ) were also studied. Photoconductivity measurement was also carried out to.

**Keywords** - Mixed crystals, Crystal growth, SXRd analysis, UV-Vis-NIR spectra, Thermal analysis, Photoconductivity, Dielectric properties.

### I. INTRODUCTION

Semiorganic nonlinear optical (NLO) materials have been investigated due to their widespread industrial potential applications in the field of optoelectronics, photonics, telecommunication, optical computing, optical storage and optical information process [1]. Nowadays organic and inorganic materials are being replaced by semi organics. They share the properties of both organic and inorganic materials. The approach of combining the high nonlinear optical materials of the organic molecules with physical properties of the inorganics has been found to be overwhelmingly successful in the recent search. Hence the recent search is concentrated on semiorganic materials due to their large nonlinearity, high resistance to laser induced damage, low angular sensitivity and good mechanical hardness [2,3]. These versatile behaviours of amino acid based semiorganic crystal attract the researchers.

There are several amino acids crystals that seem to be promising material as a nonlinear optical generator. Progress in these areas would be greatly enhanced by the availability of materials compatible with various device embodiments and having sufficiently large NLO response. Hence, new types of NLO materials have been built from organic-inorganic complexes in which the high optical nonlinearity of a purely organic compound is combined with the favourable mechanical and thermal

properties of inorganic materials. Complexes of amino acids with inorganic acids and salts are promising materials for optical second harmonic generation (SHG), as they tend to combine the advantages of the organic amino acid with that of the inorganic acid. Naturally amino acids exhibit chiral properties and crystallize in the non-centro symmetric space group [4,5]. Amino acid has both a proton donating carboxyl group ( $\text{COO}^-$ ) and a proton accepting amino group ( $\text{NH}_3^+$ ) [6]. Hence the salts of amino acids like L-arginine, L- histidine, L- alanine have been studied for NLO application [7-11]. Semi organic material such as L- histidine hydrochloride monohydrate [LHHC], L-histidine bromide (LHB), L- valanine hydrochloride, L-arginine hydrochloride are some suitable material for NLO application [12-13].

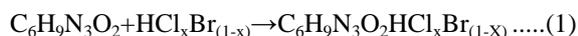
L-argininium hydrochloride bromide (LAHCIBr) is one among the recently developed amino acid crystals of the L-arginine family. LAHCIBr is a mixed crystal, with two different anions in the crystal lattice. A mixed crystal can be generally obtained by mixing two isomorphous crystals. LAHCl and LAHBr are two ideal crystals for the formation of mixed system, which satisfy all the above conditions [14]. More recently, L-histidine has been extensively studied because of the ability of its imidazole moiety to act as a proton donor, a proton acceptor and a nucleophilic agent [15]. In view of this, several reports are available on individual single

crystals of L-histidine hydrochloride(LHC) and L-histidine hydrobromide(LHB). But, there is no report available on the two component LHC-LHB mixed single crystals. In the present investigation, mixed LHC- LHB crystals with different ratios (a total of ten crystals including the two end members) were grown and characterized by SXRD, UV-Vis-NIR spectral, TG-DTA, SHG, dielectric and photoconductivity measurements. The results obtained are reported herein and discussed.

## II. EXPERIMENTAL PROCEDURE

### 2.1 Growth of LHC-LHB single crystals

Analytical reagent (AR) grade L-histidine, hydrochloric acid(HCl) and hydrobromic acid(HBr) were used along with double distilled water for the growth of sample crystals. Equimolar proportion of L-histidine and acid( $HCl_xBr_{1-x}$ ) were mixed and stirred well for about three hours to reach homogeneity. The resultant solution was filtered twice and transferred to a beaker and allowed to evaporation. A total of ten crystals were grown with x having the values 0.0 (pure LHB), 0.2, 0.3, 0.4, 0.5, 0.6, 0.7, 0.8, 0.9 and 1.0 (pure LHC). The composition of the chemicals used for the synthesis of different crystals for this study follows the chemical equation(1)



Here, x is the molar concentration (< 1.0). To ensure high purity, the material was purified by successive crystallization. The super saturated solutions of the above synthesised salt was prepared and left for slow evaporation. Transparent good quality crystals were grown in a period of about 25 days.

### 2.2 Characterization

Single crystal X-ray diffraction (SXRD) analysis has been carried out by using an ENRAF NONIUS CAD4 X-ray diffractometer with  $MoK_{\alpha}$  ( $\lambda=0.7107 \text{ \AA}$ ) radiation to identify the crystal system and to estimate the lattice parameters of the grown crystals. UV-Vis-NIR spectra of crystal samples were recorded in the wavelength region between 190 and 1100 nm by using a Shimadzu UV-1061 UV-Vis-NIR Spectrophotometer. SHG efficiency of the crystals was determined by the powder technique developed by Kurtz and Perry [16] using a Q-switched, mode locked Nd: YAG laser emitting 1.06  $\mu\text{m}$ , 8 ns laser pulses with spot radius of 1 mm. Thermogravimetric (TGA) and differential thermal(DTA) analyses were carried out between 28 and 1000 °C at a heating rate of 15 °C/min using the instrument NETZSCH STA 409C. Vickers hardness measurements were carried out using a Leitz Wetzlar

Vickers microhardness tester. The photo and dark currents were measured by using a picoammeter (Keithley 485) for various applied electric fields ranging from 0-1500 V/cm.

Dielectric measurements were made following the methods adopted by Mahadevan and his co-workers[17-19] at various temperatures ranging from 40-90°C with five different frequencies, viz.100 Hz, 1 kHz, 10 kHz, 100 kHz and 1 MHz using a HIOKI 3532-50 LCR HITESTER . The observations were made while cooling the sample. The dimensions of the crystals were measured using a travelling microscope. Air capacitance ( $C_{air}$ ) was also measured. The crystals were shaped and polished and the opposite faces were coated with graphite to form a good ohmic contact. The sample was mounted between the silver electrodes and annealed at 90°C for about 30 min to homogenize the sample before making observations.

As the crystal area was smaller than the plate area of the cell, the real part of the dielectric constant was estimated using Mahadevan's relation[20-22]

$$\epsilon' = [A_{air}/A_{cry}][C_{cry} - (C_{air} (1-A_{cry}/A_{air}))/C_{air}] \dots (2)$$

where  $C_{cry}$  is the capacitance with crystal (including air),  $C_{air}$  is the capacitance of air,  $A_{cry}$ , is the area of the crystal touching the electrode and  $A_{air}$  is the area of the electrode. The imaginary part of the dielectric constant ( $\epsilon''$ ) was calculated with the measured dielectric loss factor ( $\tan \delta$ ) using the relation

$$\epsilon'' = \epsilon' \tan \delta \dots (3)$$

The AC electrical conductivity ( $\sigma_{ac}$ ) was calculated using the relation

$$\sigma_{ac} = \epsilon_0 \epsilon \omega \tan \delta \dots (4)$$

Where  $\epsilon_0$  is the permittivity of free space ( $8.85 \times 10^{-12} \text{ C}^2\text{N}^{-1}\text{m}^{-2}$ ) and  $\omega$  is the angular frequency ( $\omega = 2\pi f$ ; f is the frequency of the applied electric field).

## III. RESULTS AND DISCUSSION

### 3.1 Crystals grown and lattice parameters

A photograph of the grown crystals is shown in Fig. 1. The crystals formed are non-hygroscopic in nature. Morphologies of the mixed crystals grown are not very similar to that of pure LHC and LHB crystals. However, it is found that all the crystals grown are colourless and transparent. The grown single crystals are represented as LHB, LHCB1, LHCB2, LHCB3, LHCB4, LHCB5, LHCB6, LHCB7, LHCB8 and LHC respectively when x = 0.0, 0.2, 0.3, 0.4, 0.5, 0.6, 0.7, 0.8, 0.9 and 1.0. SXRD analysis confirms that all the grown crystals belong to

the orthorhombic crystal system with non-centro symmetric space group of  $P2_12_12_1$ . The estimated lattice parameters for the end members (LHC and LHB) are found to be in good agreement with the reported values [7, 23]. The unit cell dimensions obtained by single crystal XRD study for the grown crystals are given in Table 1. There is a slight variation in the lattice parameters depending upon the proportion of mixing indicating that the formation of mixed crystals is proper. It may be the possibility of lattice variation due to the mixing of chlorine and bromine. However, the total crystal system and space group were not changed from the original orthorhombic system and  $P2_12_12_1$  space group.

### 3.2 Optical and mechanical properties

UV-Vis-NIR absorption spectrum gives information about the structure of the molecule

because the absorption of UV and visible light involves promotion of electrons in the  $\sigma$  and  $\pi$  orbitals from the ground state to higher states. Fig. 2 shows the UV-Vis-NIR absorption spectra observed in the present study. All the grown crystals exhibit a low UV cut-off wavelength below 300 nm (see Table 2) with very low absorption in the visible region indicating that these crystals can be considered as promising nonlinear optical (NLO) crystals.

The efficiency of second harmonic generation (SHG) signals were obtained for all the grown crystals with reference to KDP (53 mV). It is observed that the SHG efficiency (see Table 2) increases with increase in chlorine content and maximum for  $x = 0.5$  composition (LHCB4) and thereafter decreases. This may be attributed to the maximum entropy in the intermediate composition.

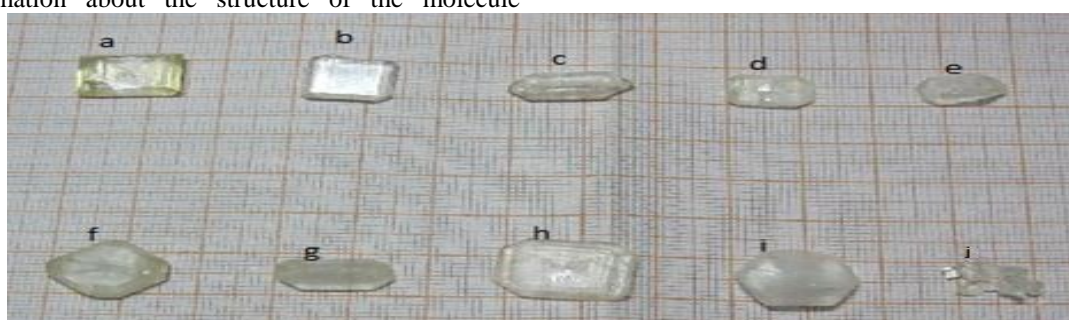


Fig. 1 Photograph of grown single crystals (a) LHC, (b) LHB, (c) LHCB1, (d) LHCB2, (e) LHCB3, (f) LHCB4, (g) LHCB5, (h) LHCB6, (i) LHCB7 and (j) LHCB8

Table 1 : The observed lattice parameters for the crystals grown. The values available in the literature for the end members are also given for comparison

| Crystal |               | Unit cell dimensions |                   |                   | $V(\text{\AA})^3$ | $\alpha=\beta=\gamma$<br>(degrees) |
|---------|---------------|----------------------|-------------------|-------------------|-------------------|------------------------------------|
|         |               | a( $\text{\AA}$ )    | b( $\text{\AA}$ ) | c( $\text{\AA}$ ) |                   |                                    |
| LHB     | Reported[7]   | 7.053                | 9.0409            | 15.2758           | 974.067           | 90                                 |
|         | Present study | 7.023                | 9.137             | 15.132            | 971.007           | 90                                 |
| LHCB1   |               | 7.032                | 9.131             | 15.127            | 971.2924          | 90                                 |
| LHCB2   |               | 7.019                | 9.148             | 15.178            | 974.5765          | 90                                 |
| LHCB3   |               | 7.009                | 9.134             | 15.201            | 973.1712          | 90                                 |
| LHCB4   |               | 6.8685               | 8.9392            | 15.3289           | 941.18            | 90                                 |
| LHCB5   |               | 6.857                | 8.934             | 15.315            | 938.2036          | 90                                 |
| LHCB6   |               | 6.83                 | 8.875             | 15.304            | 927.6711          | 90                                 |
| LHCB7   |               | 6.826                | 8.867             | 15.29             | 925.4447          | 90                                 |
| LHCB8   |               | 6.819                | 8.841             | 15.27             | 920.5791          | 90                                 |
| LHC     | Present study | 6.82                 | 8.813             | 15.26             | 917.19            | 90                                 |
|         | Reported[23]  | 6.846                | 8.921             | 15.301            | 934.48            | 90                                 |

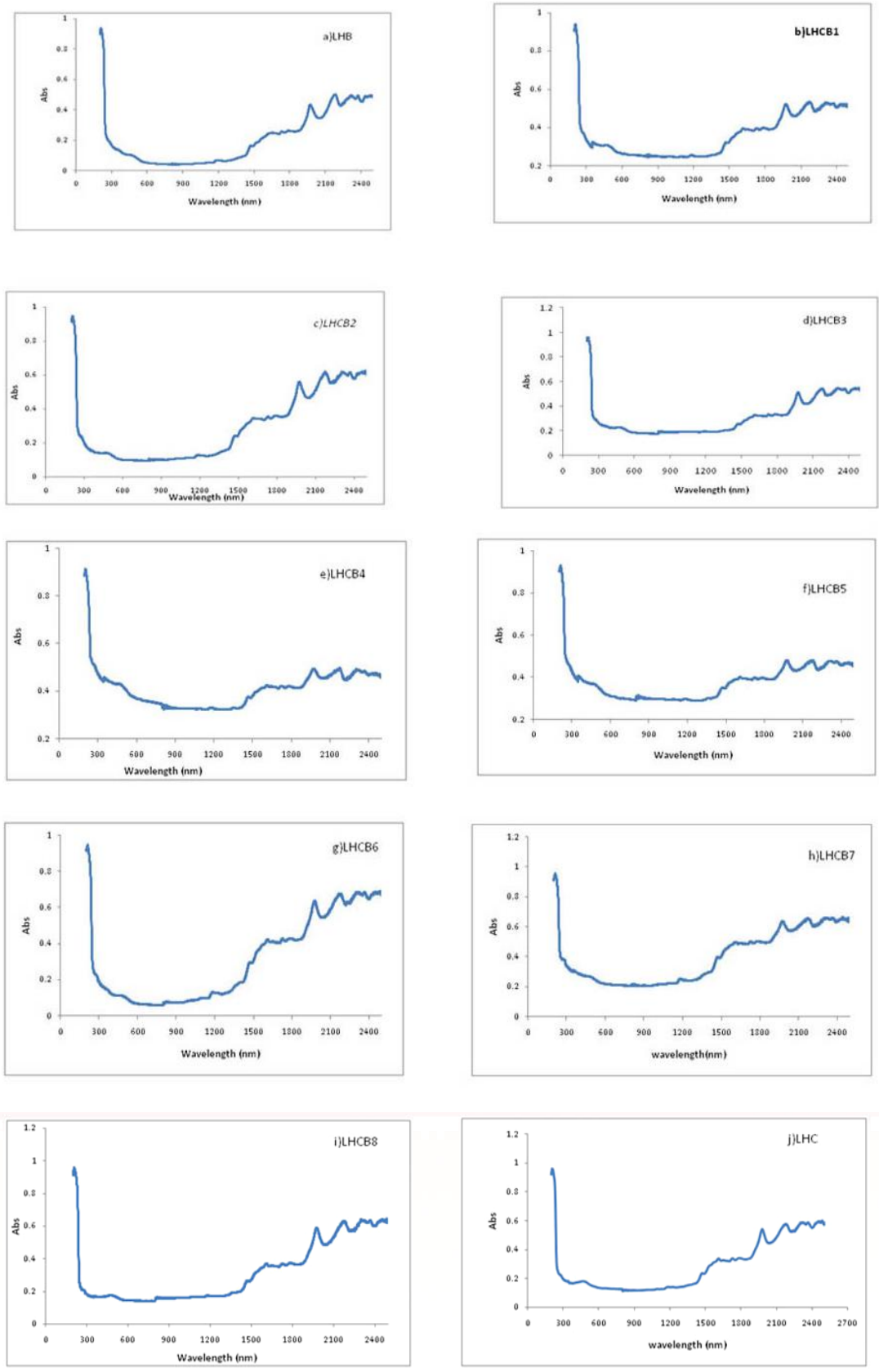


Fig. 2 UV-Vis-NIR absorption spectra observed for the grown crystals

Hardness is a measure of materials resistance to localized plastic deformation. It plays a key role in device fabrication. The variation of Vickers hardness Number (VHN) with applied load along (0 0 1) plane observed for all the grown crystals is shown in Fig. 3.

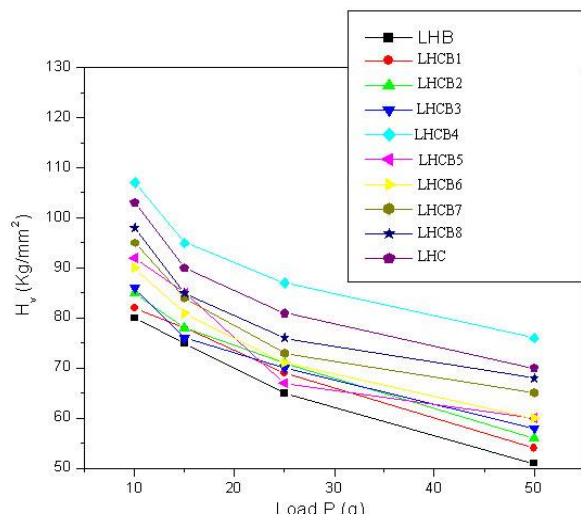


Fig. 3: Observed variation of Vickers hardness number with applied load along (0 0 1) plane

The plots indicate that the hardness decreases with increasing load. However, the hardness depends nonlinearly with the composition.

Table 2 Absorption edges, SHG efficiencies and work hardening coefficients (n) observed for the grown crystals

| Crystal  | Absorption edge (nm) | SHG efficiency (in KDP units) | n     |
|----------|----------------------|-------------------------------|-------|
| Pure LHB | 240                  | 1.22                          | 1.55  |
| LHCB1    | 270                  | 1.71                          | 1.58  |
| LHCB2    | 290                  | 1.75                          | 1.59  |
| LHCB3    | 250                  | 2.46                          | 1.616 |
| LHCB4    | 260                  | 3.53                          | 1.657 |
| LHCB5    | 270                  | 3.31                          | 1.557 |
| LHCB6    | 280                  | 3.24                          | 1.597 |
| LHCB7    | 240                  | 2.89                          | 1.617 |
| LHCB8    | 270                  | 2.93                          | 1.635 |
| Pure LHC | 280                  | 3.14                          | 1.62  |

The work hardening coefficients (n) (see Table 2) were estimated from the slopes of the best-fitted straight line plots of log p versus log d (not shown here). P is the load applied and d is the diagonal length of the indentation made on the crystal surface. According to Onitsch [24], if n > 2, the microhardness number H<sub>v</sub> increases with increasing load and if n < 2, H<sub>v</sub> decreases with increasing load. Hence the experiment results observed in the present study follow the normal indentation size effect trend.

### 3.3 Thermal properties

The TG-DTA traces of the grown crystals are shown in Fig. 4. The thermograms of all the grown crystals appear almost similar with three stages of decompositions between 130 and 410 °C followed by four stages of weight loss.

Fig. 4(a) shows the TGA and DTA thermograms of LHB crystal indicating the four stages of weight loss: the first one at 138° C and the second at 249°C, the third at 347°C and the fourth at 397°C. The total weight loss of these states corresponds to 58%. Hence it is assigned to decomposition stage of LHB crystal. The resulting residue gives a weight loss for a wider range of temperature between 600 and 750 °C. The total weight loss of this stage is found to be 38 %. As the total weight loss in the entire temperature range considered corresponds to 100%, no residue is observed. There is a sharp weight loss at 148 °C due to loss of lattice water. There are sharp endothermic peaks at 148, 257 and 342 °C and all of these coincide with the decompositions shown in the TGA trace. Fig. 4(j) shows the TGA and DTA thermograms of LHC crystal which indicates the four stages of weight loss. The first stage between 194 and 298°C with a total weight loss of 18% is assigned to the decomposition of LHC. There is a sharp endothermic peak at 198° C. It coincides with the first stage of weight loss in the TGA trace. There is one more sharp endothermic peak at 301 C. This corresponds to the second stage of weight loss in the TGA trace (298 °C). It is evident that the decomposition of the compound is taking place in four different stages.

The TGA and DTA traces of mixed crystals appear to be similar to that of end member crystals. The TGA curves indicate a major weight loss starting at about 145°C and ending at about 186°C due to elimination of volatile substances probably carbon dioxide, ammonia and oxides of chlorine. Since this temperature is beyond 100 °C, there is no evidence for any entrapped water in the crystal lattice or any physically adsorbed water on the surface of the crystal.

The thermal stability is found to gradually increase with increasing chlorine concentration (138, 145, 151, 157, 161, 169, 175, 180, 186 and 194 °C respectively when x = 0.0, 0.2, 0.3, 0.4, 0.5, 0.6, 0.7, 0.8, 0.9 and 1.0). The decomposition temperature is also shifted to higher value as a result of chlorine concentration. The results obtained indicate that these crystals are thermally stable at least up to 138 °C and establish their suitability to withstand high temperatures in laser experiments.

### 3.4 Dielectric properties

Studies on the temperature and frequency dependences of dielectric parameters, viz. dielectric

constant, dielectric loss factor and AC electrical conductivity unveil useful information about structural changes, defect behaviour, and transport

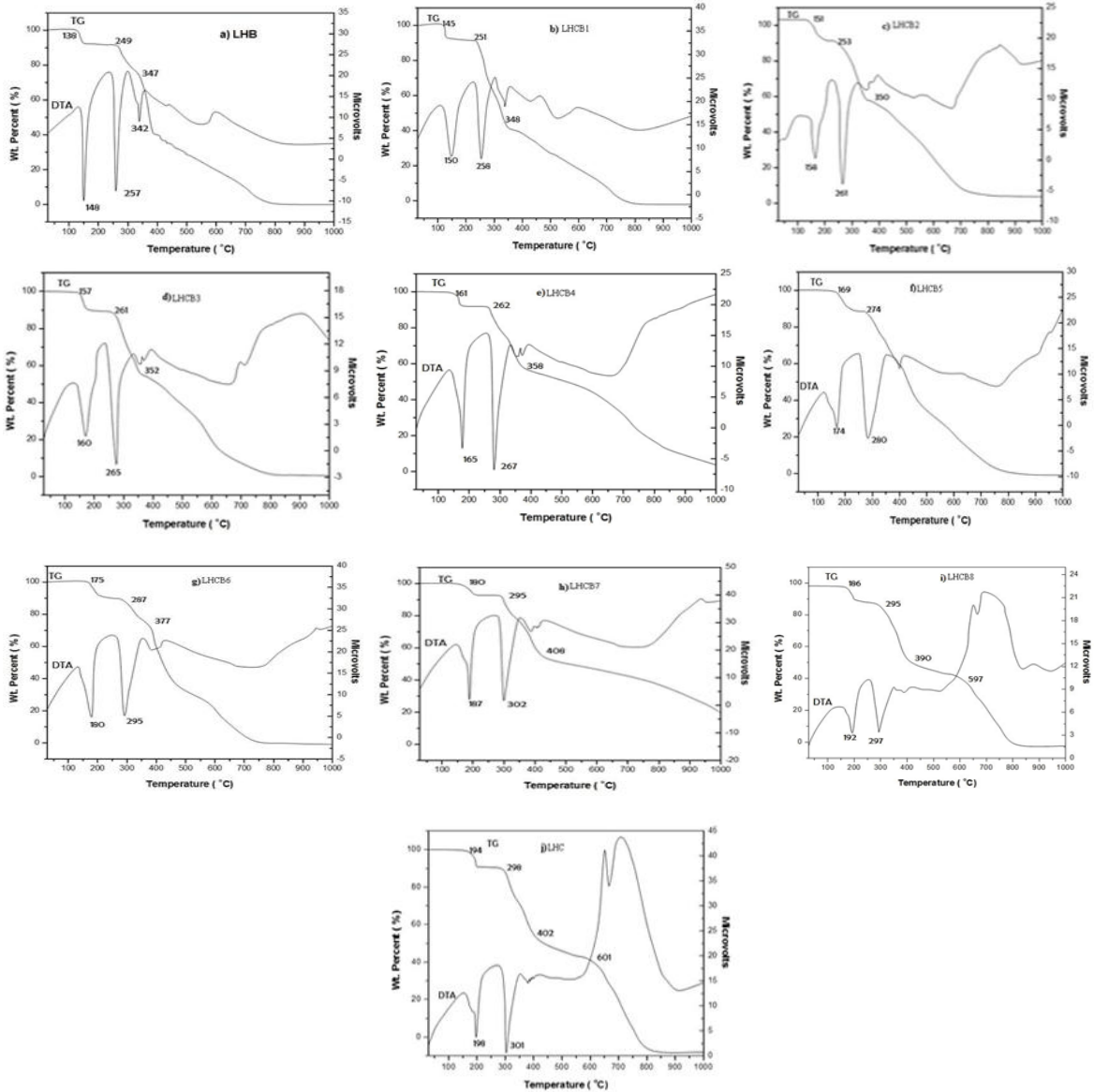


Fig. 4 TGA and DTA curves of pure LHC,LHB and mixed LHC-LHB single crystals

Table 3 AC Activation Energies Observed for the grown crystals

| Crystal | AC activation energy ( eV) |          |            |            |           |
|---------|----------------------------|----------|------------|------------|-----------|
|         | f=100 Hz                   | f= 1 kHz | f = 10 kHz | f =100 kHz | f = 1 MHz |
| LHC     | 0.181                      | 0.2233   | 0.2623     | 0.2805     | 0.2184    |
| LHB     | 0.210                      | 0.226    | 0.276      | 0.365      | 0.364     |
| LHCB1   | 0.287                      | 0.244    | 0.203      | 0.277      | 0.218     |
| LHCB2   | 0.296                      | 0.260    | 0.238      | 0.274      | 0.214     |
| LHCB3   | 0.223                      | 0.178    | 0.246      | 0.233      | 0.205     |
| LHCB4   | 0.273                      | 0.264    | 0.284      | 0.395      | 0.313     |
| LHCB5   | 0.197                      | 0.242    | 0.162      | 0.232      | 0.164     |
| LHCB6   | 0.224                      | 0.230    | 0.278      | 0.410      | 0.186     |
| LHCB7   | 0.403                      | 0.306    | 0.295      | 0.258      | 0.171     |
| LHCB8   | 0.309                      | 0.303    | 0.372      | 0.382      | 0.194     |

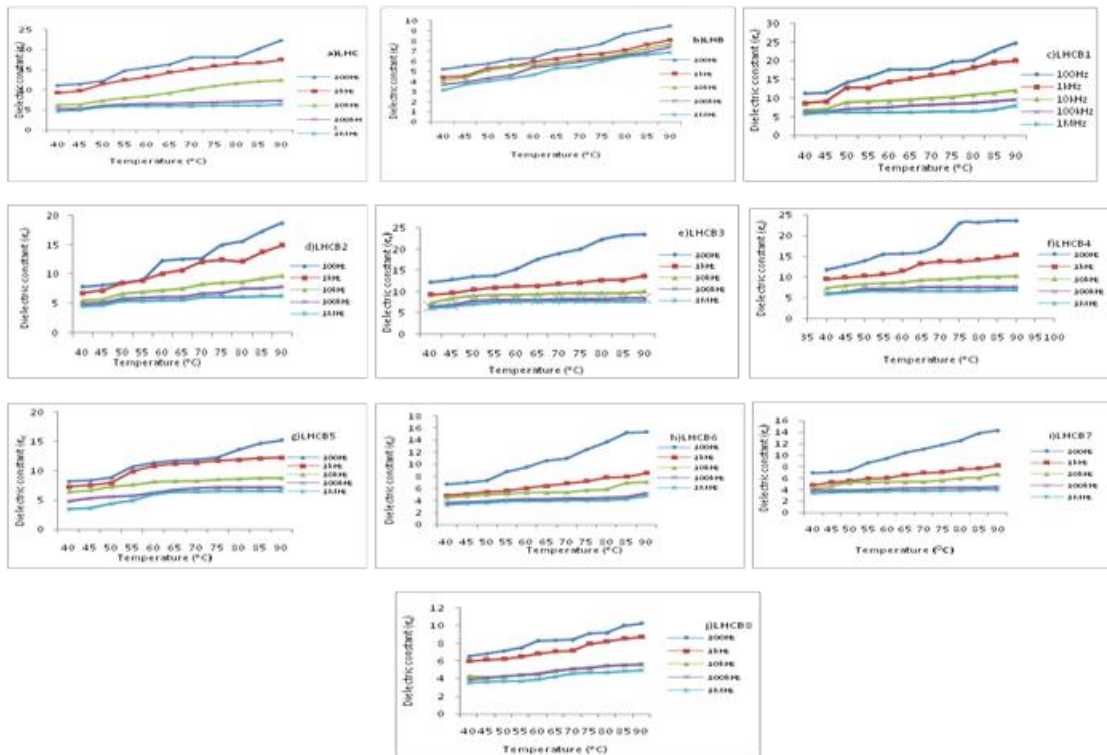


Fig. 5 : Dielectric constants observed for the grown crystals

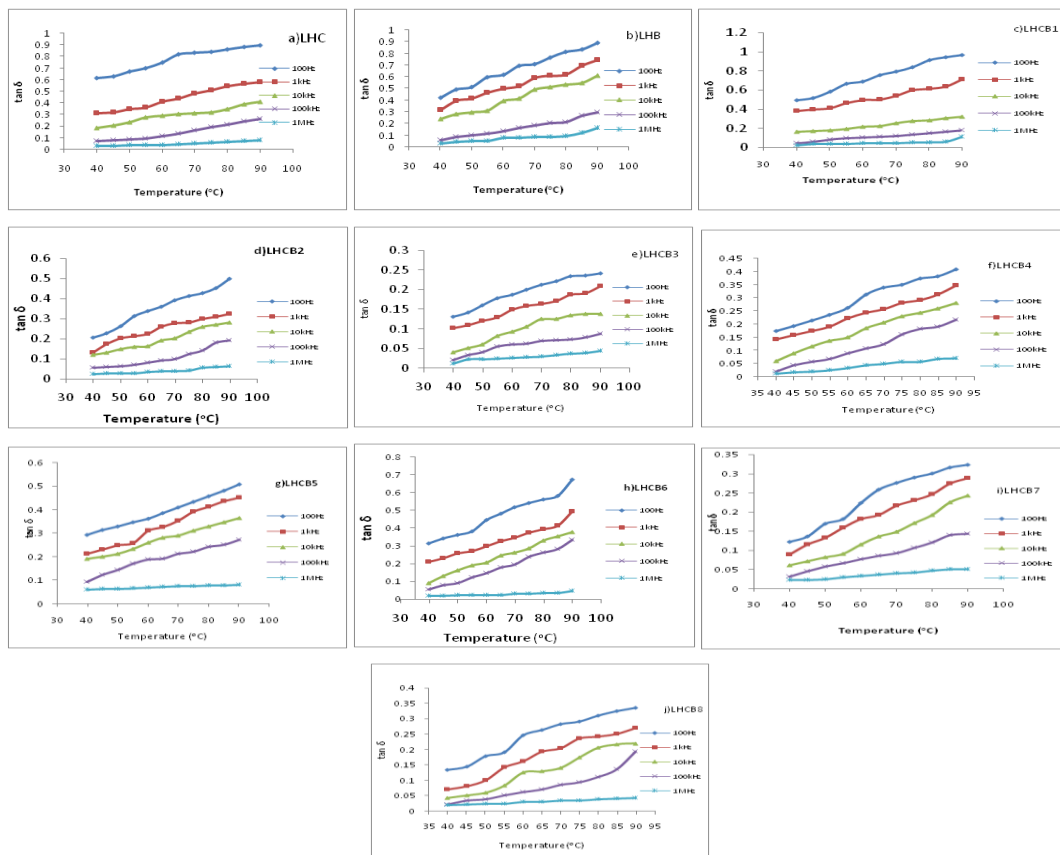


Fig. 6 : Temperature Dependence of Dielectric loss for pure LHC, LHB and mixed LHC-LHB single crystals

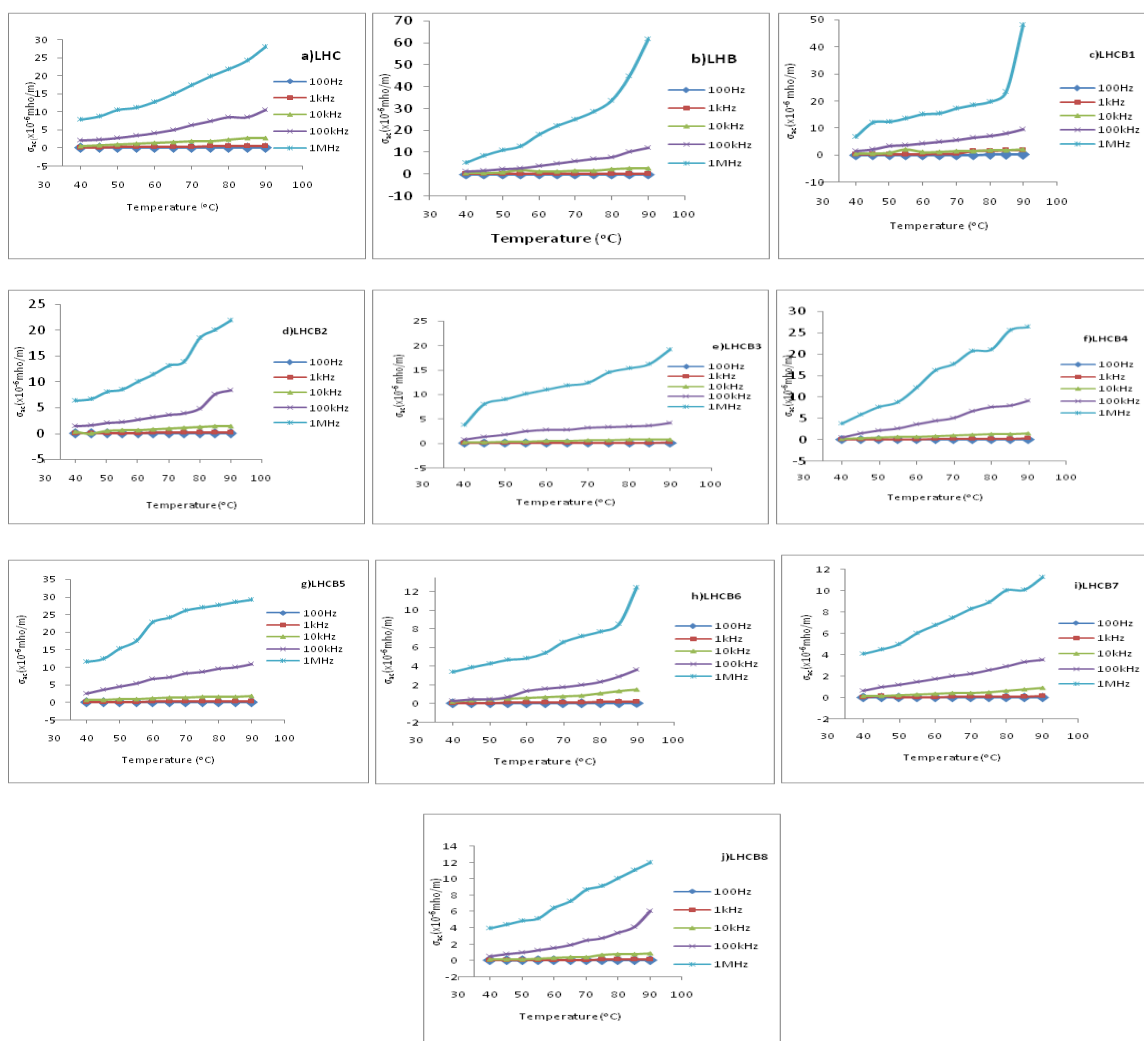


Fig. 7 The AC Electrical conductivities for pure LHC, LHB and mixed LHC-LHB single crystals

phenomenon. Figs 5-7 show the temperature and frequency dependences of dielectric parameters observed for the LHC-LHB crystals. These plots exemplify the fact that the dielectric constant and the dielectric loss are both inversely proportional to the frequency and directly proportional to the temperature. The AC conductivity is directly proportional to both frequency and temperature. This is a normal dielectric behaviour [25]. Dielectric properties are correlated with the electro-optic property of the crystals [26]. The higher values of dielectric loss ( $\tan \delta$ ) and dielectric constant observed at lower frequencies may be attributed to space charge polarization owing to charged lattice defects [27]. The considerable low value of dielectric constants observed for the grown crystals is important for extending the material applications towards photonic, electro-optic and NLO devices. Moreover, the low dielectric losses observed indicate that the crystals grown in the present study are of good quality. The AC conductivity plots indicate a typical

behaviour of most of the solid samples. Plots between  $\ln(\sigma_{ac})$  and  $1000/T$  (not shown here) were found to be very nearly linear. Activation energies were estimated using the slopes of these plots;  $[E = -(\text{slope}) k \times 1000]$ . The observed activation energies are provided in Table 3. The low activation energies observed in the temperature range considered indicate the presence of oxygen vacancies in the crystals. All dielectric loss factor, AC electrical conductivity and activation energy are found to vary nonlinearly with the composition which may be due to the random disturbance in the hydrogen bonding system due to mixing in the mixed crystals considered in the present study. The conduction mechanism can be established as due to protonic transport as in the case of potassium di-hydrogen orthophosphate (KDP) [21]. Also, the temperature dependence of AC electrical conductivity and dielectric constant can be explained as due to the temperature dependence of protonic movement and ionic polarizability respectively.

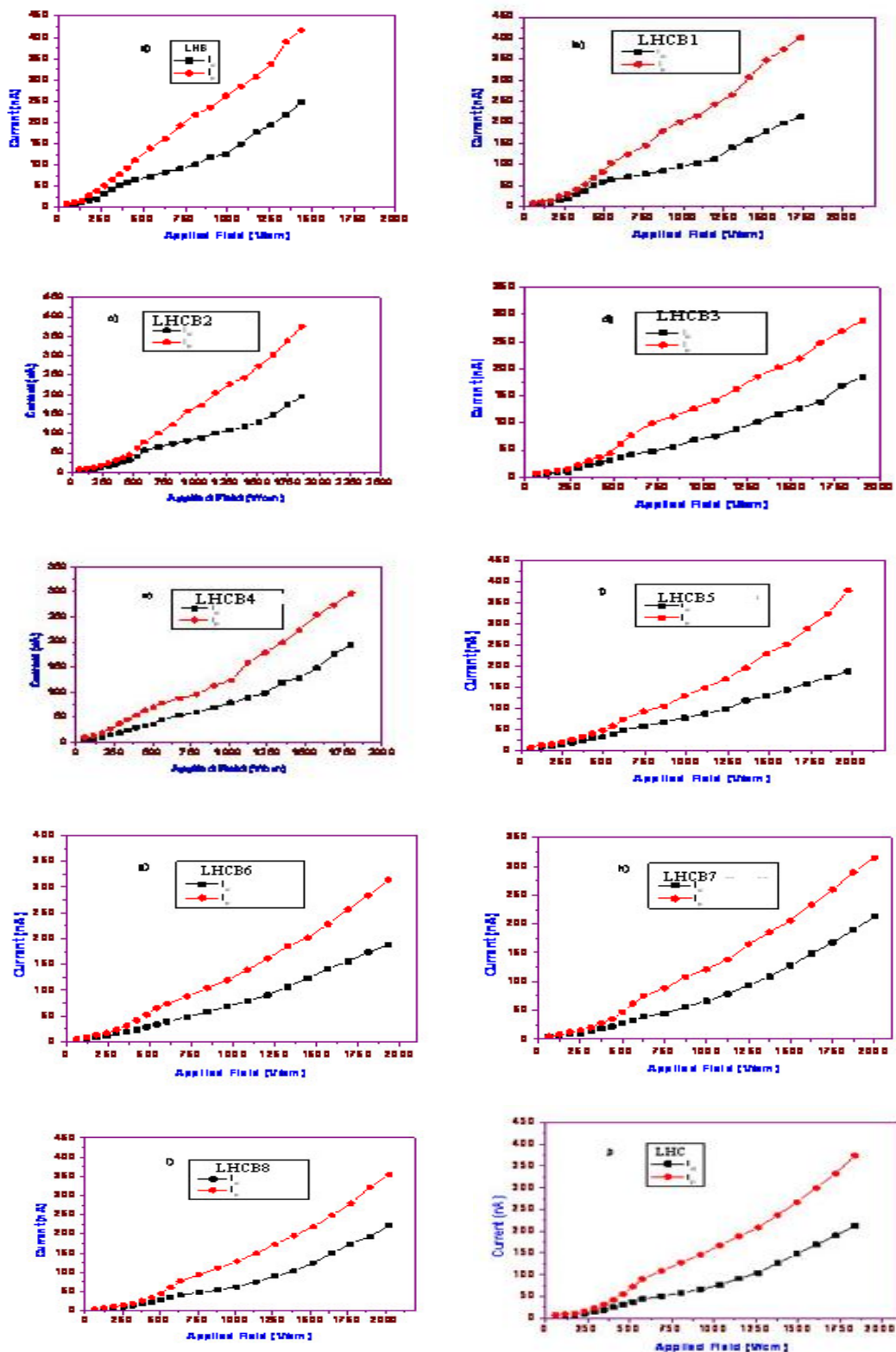


Fig. 8 Results of Photoconductivity measurements

### 3.5 Photoconductivities

The observed variation of photo current ( $I_{ph}$ ) and dark current ( $I_d$ ) with applied field is shown in

Fig. 8. Both the photo and dark currents observed for all the grown crystals increase almost linearly with the applied field. It is observed that the dark current

is less than the photo current indicating that all the grown crystals exhibit positive photoconductivity. In general, positive photoconductivity is attributed to generation of mobile charge carriers caused by the absorption of photons [28].

#### IV. CONCLUSION

Single crystals of pure LHC, pure LHB and mixed LHC-LHB(with eight compositions) have been successfully grown by the slow evaporation technique and characterised structurally, optically, mechanically and electrically. The grown crystals are optically transparent with well defined morphologies. SXRD analysis confirms that all the ten grown crystals belong to orthorhombic crystal system with space group  $P2_12_12_1$ . The low UV cut-off wavelengths observed (below 300 nm) indicate that these crystals can be considered as promising candidates for NLO applications. The powder SHG analysis reveals that the efficiency of LHCB4 material is 3.53 times that of KDP. The microhardness measurement indicates that the grown crystals are sufficiently hard and exhibit normal size indentation effect. All the grown crystals are found to be thermally stable at least up to 138 °C. A result of dielectric measurement indicates a normal dielectric behaviour. The observed dielectric constants and AC electrical conductivities have been understood as due to ionic polarizability and protonic transport. The photoconductivity study ascertains the positive photoconducting nature of all the grown crystals. The present study, in effect, indicates the possibility of forming LHC-LHB mixed crystals which can be considered as potential materials for photonic, electro-optic and SHG device applications.

#### REFERENCES

- [1] P.N. Prasad, D.J. Williams, *Introduction to nonlinear optical effects in molecules and polymers*, John Wiley Interscience, New York.(1991).
- [2] S.P. Velsko, *Laser program Annual Report*, Lawrence UCRL-JC-105000 (Lawrence Livermore National Laboratory, Livermore, California.1990)
- [3] L.F.Warren, proceedings of the Fourth International SAMPE Electronics Conference, (ed.) R.E.Allred, R.J.Martinez and W.D.Wischmann (society for the advancement of material and process engineering, Covina, ca., 4(1990)388.]
- [4] Bhat M. N. and Dharmaprakash S. M., *J. Cryst. Growth*, Vol. 235,2002, pp. 511.
- [5] Bhat M. N. and Dharmaprakash S. M. 'Growth of optical nonlinear  $\gamma$ -glycine crystals' *J. Cryst. Growth* Vol.236,2002, pp. 376-380.
- [6] Petrosyan H.A, Karapetyan H.A., Antipin M. Yu., Petrosyan A.M.,s'Nonlinear optical crystals of L-histidine salts' *J. Cryst. Growth*, Vol. 275,2005, pp 1919.
- [7] Ittyachan R. and Sagayaraj P., 'Growth and Characterization of a new promising NLO L-histidine bromide crystal' *J. Cryst. Growth*, Vol. 249,2003, pp.557-560.
- [8] Rajendran K. V., Jayaraman D., Jayavel R., and Ramasamy P.,s'Growth and characterization of L-HFB nonlinear optical crystal; L- histidinium bromide' *J. Cryst. Growth*, Vol. 255,2003(b), pp 361-368.
- [9] Ittyachan R. and Sagayaraj P.,s'Growth and characterization of L-arginine diphosphate crystals' *J. Cryst. Growth*, Vol. 243,2002,pp. 356.
- [10] Rajendran K. V., Jayaraman D., Jayavel R., and Ramasamy P.,'Effect of pH on the growth and characterization of L-HFB single crystal' *J. Cryst. Growth*, Vol. 254, 2003(a)pp. 461-468.
- [11] Dhanuskodi S. and Vasantha K., 'Structurall. Thermal and optical characterizations of NLO material: L-alaninium oxlate'. *Cryst. Res. Technol.*Vol. 39, 2004, pp. 259-265.
- [12] PanduranganAnandan, RamasamyJayavel,'Crystal growth and characterization of semiorganic single crystals of L-histidine family for NLO applications' *J. Cryst. Growth*, Vol. 322, 2011,pp 69-73.
- [13] Kirubavathi K., Selvaraju K., Valluvan R., Vijayan N., Kumararaman S.,'Synthesis, growth, strictira, spectroscopic and optical studies of a new semiorganic nonlinear optical crystal L-valine hydrochloride' *ActaCryst A*, Vol.69,2008, pp.1283-1286.
- [14] Tanusri Pal, TanusreeKar, Xin-Qiang Wang, Guang-Ying Zhou, Dong Wang, Xiu-Feng Cheng, Zhao-He Yang, ,'Growth and characterization of non linear optical material,LAHClBr- a new member of L-arginine halide family'. *J. Crystal Growth* Vol.235, 2002, pp.523-528.
- [15] Madden J.J, Edward L. McGandy, Nadrian C. Seeman, *Acta (1972)Cryst B*, 28, 2377.
- [16] Kurtz S.K., Perry T.T.,'A powder technique for the evaluation of nonlinear optical materials', *J. Appl. Phys*, Vol.39,1968,pp. 3798-3813.
- [17] Manonmani N., Mahadevan C.K., Umayorubhagan V. Growth and studies of the new crystal formed with NaCl andCaCl<sub>2</sub> , *Mater.Manuf.Processes*,22, 2007,388-392
- [18] Priya M., Mahadevan C.K. Preparation and dielectric properties of oxide added NaCl-KCl polycrystals, *Physica B*,403, 2008,67-74
- [19] Mahadevan C.K., Jayakumari K.(2008) Electrical measurements on multiphased (NaCl)<sub>x</sub>(KCl)<sub>y</sub>-x(KBr)<sub>1-y</sub> single crystals, *Physica B*,403, 2008,3990-3996

- [20] Goma S., Padma C.M., Mahadevan C.K. (2006) Dielectric parameters of KDP single crystals added with urea, *Mater.Lett.*,60, 2006,3701-3705
- [21] Meena M., Mahadevan C.K., Growth and electrical characterization of L-arginine added KDP and ADP single crystals, *Cryst.Res.Tech.*,43,2008, 166-172
- [22] Meena M., Mahadevan C.K., Growth and dielectric properties of L-arginine acetate and L-arginine oxalate single crystals, *Mater.Lett.*,62,2008, 3742-3744
- [23] Oda K. and Koyama H., *Acta Cryst. B*, Vol. 28,1972,pp. 639.
- [24] Onitsch E.M., 'The present status of testing the hardness of materials', *Mikroskopie*, Vol..95 95, 1956,pp. 12-14.
- [25] Anderson J.C., 'Dielectrics', Chapman and Hall, London1964 .
- [26] Boomadevi S. and Dhanasekaran R., 'Synthesis, crystal growth and characterization of L-pyrrolidone -2- carboxylic acid (L-PCA) crystals', *Journal of Crystal Growth*, Vol. 261, 2004,pp. 70-76.
- [27] Vasudevan A., Carin S., Melloch M.R. and Hannon E.S., 'Permittivity of GaAs epilayers containing arsenic precipitates' *Applied Physics Letters*, Vol. 73, 1998,pp. 671.
- [28] Joshi V.N., 'Photoconductivity', Marcel Dekker, New York1990.